

# The Feasibility of Formation and Kinetics of NMR Signal Amplification by Reversible Exchange (SABRE) at High Magnetic Field (9.4 T)

Danila A. Barskiy,<sup>†,‡</sup> Kirill V. Kovtunov,<sup>†,‡</sup> Igor V. Koptyug,<sup>†,‡</sup> Ping He,<sup>∇</sup> Kirsten A. Groome,<sup>∇</sup> Quinn A. Best,<sup>∇</sup> Fan Shi,<sup>∇</sup> Boyd M. Goodson,<sup>∇</sup> Roman V. Shchepin,<sup>§</sup> Aaron M. Coffey,<sup>§,||</sup> Kevin W. Waddell,<sup>§,⊥</sup> and Eduard Y. Chekmenev<sup>\*,§,||,#</sup>

<sup>†</sup>International Tomography Center, <sup>‡</sup>Novosibirsk State University, Novosibirsk 630090, Russia

<sup>§</sup>Institute of Imaging Science, Department of Radiology, <sup>||</sup>Department of Biomedical Engineering, <sup>⊥</sup>Department of Physics and Astronomy, <sup>#</sup>Department of Biochemistry, Vanderbilt University, Nashville, Tennessee, 37232-2310, United States

<sup>∇</sup>Department of Chemistry and Biochemistry, Southern Illinois University, Carbondale, Illinois 62901, United States

## S Supporting Information

**ABSTRACT:** <sup>1</sup>H NMR signal amplification by reversible exchange (SABRE) was observed for pyridine and pyridine-*d*<sub>5</sub> at 9.4 T, a field that is orders of magnitude higher than what is typically utilized to achieve the conventional low-field SABRE effect. In addition to emissive peaks for the hydrogen spins at the ortho positions of the pyridine substrate (both free and bound to the metal center), absorptive signals are observed from hyperpolarized orthohydrogen and Ir-complex dihydride. Real-time kinetics studies show that the polarization build-up rates for these three species are in close agreement with their respective <sup>1</sup>H T<sub>1</sub> relaxation rates at 9.4 T. The results suggest that the mechanism of the substrate polarization involves cross-relaxation with hyperpolarized species in a manner similar to the spin-polarization induced nuclear Overhauser effect. Experiments utilizing pyridine-*d*<sub>5</sub> as the substrate exhibited larger enhancements as well as partial H/D exchange for the hydrogen atom in the ortho position of pyridine and concomitant formation of HD molecules. While the mechanism of polarization enhancement does not explicitly require chemical exchange of hydrogen atoms of parahydrogen and the substrate, the partial chemical modification of the substrate via hydrogen exchange means that SABRE under these conditions cannot rigorously be referred to as a non-hydrogenative parahydrogen induced polarization process.

NMR hyperpolarization techniques increase nuclear spin polarization by several orders of magnitude,<sup>1–3</sup> which leads to the corresponding increase in NMR signal enabling an array of applications including studies of catalytic processes<sup>4</sup> and biomedical use of hyperpolarized substrates as MRI contrast agents.<sup>5–8</sup> There are several hyperpolarization methods, including dynamic nuclear polarization (DNP),<sup>9</sup> spin-exchange optical pumping,<sup>10</sup> parahydrogen-induced polarization (PHIP)<sup>11</sup> using parahydrogen and synthesis allow dramatically enhanced nuclear alignment (PASADENA),<sup>12</sup> and others. One of the newest methods is signal amplification by reversible exchange

(SABRE),<sup>13,14</sup> with the experiments conducted by shaking the solutions of an Ir catalyst (i.e., Crabtree's catalyst<sup>15</sup> or N-heterocyclic carbene complex<sup>16</sup>) with parahydrogen and a polarizable substrate at a relatively low magnetic field of a few mT, followed by physical transfer of the sample to the high-field NMR spectrometer. Alternatively, the *in situ* detection of SABRE effects at low magnetic fields has been demonstrated.<sup>17</sup> However, the latter approach does not provide sufficient chemical shift resolution, and therefore interpretation of the low-field NMR studies of SABRE often relies on the previous reports of *ex situ* high-field detection.<sup>13,14,18</sup> Furthermore, high-field SABRE is commonly thought to be unobservable, because of the expectation that canonical SABRE<sup>13</sup> would be quenched by the fact that the *J*-coupling mediated flip-flops would no longer be energy conserving. The control experiments in the early SABRE studies seemingly confirm these expectations.<sup>13</sup> In addition, a common misconception is that SABRE is not a chemical process since the polarized substrate appears to be chemically identical to its thermally polarized counterpart. Here, we show that generation of SABRE in high magnetic fields is possible and that the substrate is clearly involved in a chemical (hydrogen exchange) process while coordinated to a metal center. To the best of our knowledge, this is the first time the SABRE effects are generated and detected *in situ* in a high magnetic field.

The *in situ* SABRE studies of pyridine-*h*<sub>5</sub> (Py-*h*<sub>5</sub>) and pyridine-*d*<sub>5</sub> (Py-*d*<sub>5</sub>) at high field (9.4 T) were performed using methanol-*d*<sub>4</sub> solutions of N-heterocyclic carbene complex-based Ir catalyst, which shows the highest efficiency in low-field SABRE studies reported to date.<sup>19</sup> Parahydrogen gas (>90% para-state)<sup>20</sup> was bubbled through ~7 mM solutions of [IrCl(COD)(IMes)]<sup>16</sup> (IMes = 1,3-bis(2,4,6-trimethylphenyl)imidazol-2-ylidene; COD = cyclooctadiene) in perdeuterated methanol, solution (1), using 100 mM concentration of substrate, Py-*h*<sub>5</sub> or Py-*d*<sub>5</sub> (see Supporting Information (SI) for details). The <sup>1</sup>H NMR spectra were acquired immediately after the bubbling was stopped (~3 ± 2 s). This experimental approach allowed for *in situ* detection of hyperpolarized species that exist during the high-field SABRE

Received: November 15, 2013

Published: February 14, 2014

process. All NMR spectra presented here were obtained using this approach unless otherwise noted.

Figure 1c shows the  $^1\text{H}$  NMR spectrum of  $\text{Py-}h_3$  in the catalyst solution (1) using the above experimental approach after 2 min

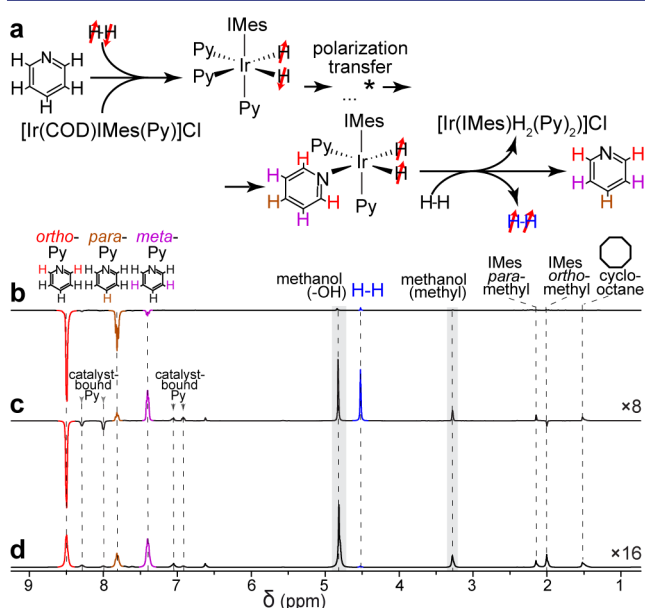


**Figure 1.** (a) Schematics of the SABRE exchange process, with asterisk to represent a potential intermediate state. (b)  $^1\text{H}$  NMR spectrum of catalyst solution (1) containing  $\text{Py-}h_3$  bubbled with parahydrogen in the fringe field of a 9.4 T magnet followed by rapid transfer to 9.4 T for high-field NMR acquisition. (c) *in situ* NMR spectrum acquired after bubbling with parahydrogen at 9.4 T, and (d) thermal NMR spectrum of solution (1) containing  $\text{Py-}h_3$  after 2 min of parahydrogen bubbling. NMR peak assignments<sup>24</sup> are also provided in SI.

of parahydrogen bubbling. For comparison, the canonical SABRE NMR spectrum of hyperpolarized  $\text{Py-}h_3$ , wherein the sample is first polarized by bubbling parahydrogen in the NMR magnet's fringe field prior to sample transfer to 9.4 T for signal acquisition, is shown in Figure 1b and demonstrates that all protons of  $\text{Py-}h_3$  are polarized. In contrast, only the signals from the ortho-protons of  $\text{Py-}h_3$  exhibit significant enhancement in the *in situ* high-field experiment. The observation of hyperpolarized ortho-H-Py is unexpected for two reasons: First, because SABRE was previously reported to be exclusively generated by parahydrogen exchange at low magnetic fields<sup>13,14</sup> and explained by level anticrossings which should be quenched at high fields;<sup>21</sup> and second, the strong selectivity for the ortho position of Py is itself counter to previous observations. Moreover, NMR spectra acquired over a conventional range of proton chemical shifts (see Figure 1c) also revealed other species with nonequilibrium polarizations: hyperpolarized orthohydrogen manifesting as a strong absorptive peak at  $\sim 4.5$  ppm and a weak emissive peak at  $\sim 2$  ppm for the ortho methyl groups of the IMes moiety of the metal complex. While hyperpolarized H-D was recently reported by Appelt et al.,<sup>17</sup> observation of hyperpolarized orthohydrogen in SABRE experiments is reported here for the first time. In retrospect, the absence of previous reports is not surprising because  $T_1$  of dissolved orthohydrogen (see below) is only 2 s or less. Thus, most studies with *ex situ* detection would likely miss the presence of hyperpolarized orthohydrogen as it would largely relax back to equilibrium level during sample transfer from the low polarizing field to the high detection field. Because of these

concerns, the hydride spectral region was also investigated, and hyperpolarized signal of the dihydride complex at  $\sim -23$  ppm was detected with signal enhancement  $\varepsilon \sim 200$  (calculated as the ratio of the hyperpolarized signal and the thermally induced signal) and  $T_1 = 3.0 \pm 0.3$  s (Figure S2). In the previous reports, an antiphase hyperpolarization pattern was observed for the dihydride complex, but only when  $^{15}\text{N}$ -labeled pyridine was used to eliminate magnetic equivalence of the two hydride ligands.<sup>13,14</sup> In contrast, here the hyperpolarized hydride resonance is purely absorptive and is observed despite the fact that the two hydride ligands are essentially magnetically equivalent. Most published SABRE studies present only the region of NMR spectra corresponding to substrate aromatic protons,<sup>18,21</sup> which may obscure the possible presence of other hyperpolarized species. Moreover, low-field *in situ* NMR studies lacking chemical shift resolution often assume that the entire signal is due to hyperpolarized substrate, while both orthohydrogen and Ir dihydride were polarized here by more than 100-fold (corresponding to nuclear spin polarizations of  $>0.3\%$ ), suggesting that previously published low-field hyperpolarized spectra may have been significantly impacted by the presence of hyperpolarized dihydride, orthohydrogen, or other species<sup>17,22</sup> rather than detecting only hyperpolarized substrate molecules.<sup>23</sup>

The *in situ* detection enabled the measurement of relaxation parameters as well as the kinetics of hyperpolarization build-up. The former was measured using a series of time-resolved NMR spectra acquired using small angle excitation RF pulses (Figures 2b,d,f and 3b,d,f). The  $T_1$  values of hyperpolarized hydride and orthohydrogen could be overestimated, because residual dissolved parahydrogen may continue to react after the bubbling was stopped. The polarization dynamics was studied by varying

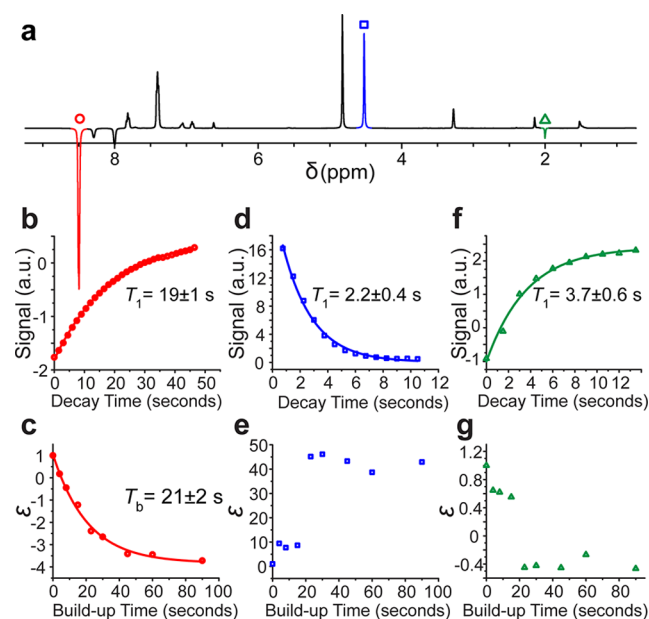


**Figure 2.** *In situ* SABRE  $^1\text{H}$  NMR spectroscopy of  $\text{Py-}h_3$  in catalyst solution (1) at 9.4 T. (a) NMR spectrum acquired after bubbling of parahydrogen at 9.4 T. (b,d,f)  $T_1$  measurements of hyperpolarized ortho-H of  $\text{Py-}h_3$ , orthohydrogen, and ortho- $\text{CH}_3$  of IMes respectively. (c,e,g) Hyperpolarization build-up curves of ortho-H of  $\text{Py-}h_3$ , orthohydrogen, and ortho- $\text{CH}_3$  of IMes respectively as a function of reaction/bubbling time.  $\varepsilon$  values are calculated by comparing hyperpolarized spectral integrals with those obtained with "normal" (thermally equilibrated) signals.

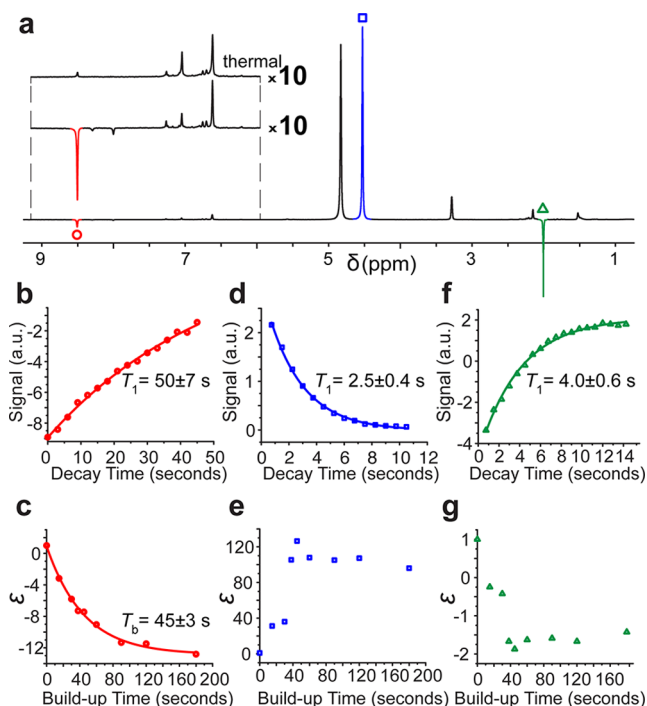


**Figure 3.** *In situ* SABRE  $^1\text{H}$  NMR spectroscopy of  $\text{Py-d}_5$  (99.96% D) at 9.4 T using catalyst solution (1). (a) NMR spectrum acquired after bubbling of parahydrogen at 9.4 T; the inset shows a close-up of a portion of the main figure, along with that of a corresponding thermal spectrum. (b,d,f)  $T_1$  measurements of hyperpolarized *ortho*-H of  $\text{Py-d}_4\text{-h}$ , orthohydrogen, and *ortho*- $\text{CH}_3$  of IMes respectively. (c,e,g) Hyperpolarization build-up curves of *ortho*-H of  $\text{Py-d}_4\text{-h}$ , orthohydrogen, and *ortho*- $\text{CH}_3$  of IMes as a function of reaction time.

the bubbling time of parahydrogen gas through solution (1) at 9.4 T (Figures 2c,e,g and 3c,e,g). The time constants for exponential polarization build-up for both  $\text{Py-h}_5$  and  $\text{Py-d}_4\text{-h}$ <sup>25</sup> are in good quantitative agreement with their  $T_1$  values to within experimental error (Figures 2 and 3). The extrapolated values for  $\epsilon$  (time  $\rightarrow \infty$ ) of hyperpolarized ortho protons of pyridine were  $-4.9$  and  $-14.7$  for  $\text{Py-h}_5$  and  $\text{Py-d}_4\text{-h}$  (Figures 2c and 3c, respectively). These results are in a qualitative agreement with the significantly increased value for  $T_1(\text{Py-d}_4\text{-h})$  compared to  $T_1(\text{Py-h}_5)$ . It should also be noted that these  $T_1$  values significantly exceed the characteristic exchange times of Py and  $\text{H}_2$  with the Ir complex of  $\sim 0.1$  s.<sup>24</sup> Taken together, these results are consistent with substrate (Py) polarization mechanism that is different from what is typically observed with canonical (low-field) SABRE—one that instead relies on nuclear spin cross-relaxation with another species with highly nonequilibrium spin order in a manner akin to the spin polarization-induced nuclear Overhauser effect (SPINOE).<sup>2,23,26</sup> In addition to the fact that the enhanced signal of the substrate would be expected to grow with a time constant similar to its autorelaxation rate, the low value expected for nuclear spin cross-relaxation rates would explain the much lower values of  $\epsilon$  compared to low-field SABRE (Figure 1b,c). Moreover, when the decay process is reduced via extending  $T_1$  ( $\text{Py-d}_4\text{-h}$  vs  $\text{Py-h}_5$ ), the  $\epsilon$  value increases significantly.

Motivated by the previous report of H-D formation<sup>17</sup> during SABRE hyperpolarization and the lack of H-D signatures in the present  $\text{Py-h}_5$  studies performed in methanol- $d_4$  (Figure 2),  $\text{Py-d}_5$  was used as a SABRE substrate (Figure 3) as well as the substrate in H/D exchange studies with “normal” (thermally equilibrated)

hydrogen gas. During the latter experiments, a low-pressure NMR tube containing solution (1) and  $\text{Py-d}_5$  (99.96% D) was allowed to react with “normal” hydrogen in the NMR magnet and monitored *in situ* with NMR spectroscopy. Although the Ir-catalyzed exchange is slow because there is no sample agitation and the reaction is diffusion limited, H-D was formed as confirmed by the observation of the characteristic splitting  $J_{\text{HD}} = 42.8$  Hz in the  $^1\text{H}$  NMR spectrum, Figure 4c.<sup>17,27</sup> Moreover, the

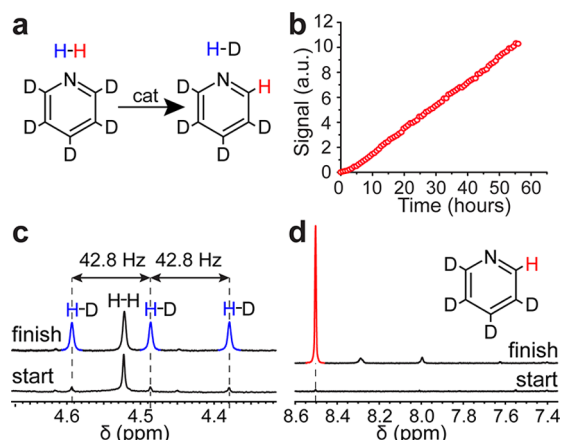


**Figure 4.** Deuterium exchange studies using  $\text{Py-d}_5$  (99.96%D) at 1 atm. (a) Scheme of deuterium exchange of  $\text{Py-d}_5$  and  $\text{H}_2$  (note that only the *ortho*- position exhibits exchange). (b) The build-up curve of the *ortho*-H signal of  $\text{Py-d}_4\text{-h}$ . (c)  $\text{H}_2$  region of NMR spectra of the Ir catalyst mixed with  $\text{Py-d}_5$  and “normal”  $\text{H}_2$ <sup>32</sup> in a sealed NMR tube at room temperature at the start and finish of  $\sim 56$  h exchange process during NMR experiments monitoring this exchange process. Note the characteristic  $J_{\text{HD}} = 42.8$  Hz.<sup>27</sup> (d) *ortho*-H-Py region of NMR spectra of the Ir catalyst mixed with  $\text{Py-d}_5$  and “normal”  $\text{H}_2$  in a sealed NMR tube at room temperature at the start and finish of NMR experiments monitoring the exchange process.

signal from the *ortho*-proton of  $\text{Py-d}_4\text{-h}$  was increasing steadily during the extended reaction period (Figure 4b,d). Furthermore, the presence of H-D was also detected in the thermal spectra after bubbling parahydrogen through solution (1) containing 100 mM  $\text{Py-d}_5$ , Figure S3, but not in solution (1) containing 100 mM  $\text{Py-h}_5$ , confirming that the source of deuterium in the formed H-D is indeed the substrate  $\text{Py-d}_5$  rather than the deuterated solvent methanol- $d_4$ . This result is not consistent with the observation by Appelt et al.,<sup>17</sup> who concluded that H-D was formed with deuterium atoms coming from the solvent. This discrepancy is likely explained by their use of a different, i.e., Crabtree’s, catalyst<sup>17</sup> compared to the  $[\text{IrCl}(\text{COD})(\text{IMes})]$ <sup>16</sup> catalyst used here. Similar H/D exchange with  $\text{H}_2/\text{D}_2$ <sup>28</sup> and alcohols<sup>29</sup> was described earlier.

While the H/D exchange described here is unlikely to contribute substantially to the hyperpolarization process, it is happening concurrently with SABRE. These exchange studies (Figure 4) clearly demonstrate that the  $\text{Py-d}_5$  substrate is being modified as a result of this chemical exchange process. Therefore, this process cannot rigorously be referred to as an exclusively non-hydrogenative (NH)-PHIP,<sup>30</sup> because at least some fraction of the substrate undergoes chemical modification when parahydrogen is used as a source of hyperpolarization. The contribution of this process may crucially depend on the nature of the metal complex, the substrate, and experimental conditions and thus should not be dismissed without careful consideration.

The observations of SABRE formed in a high field, hyperpolarized (absorptive) orthohydrogen and hydride signals, and the deuterium-proton exchange process differ with previously published studies.<sup>13,18</sup> The discrepancy may be explained in part by the limitations of the design of the typical control experiments, for instance, where high-field *in situ* detection was not available or the deuterium exchange was not studied thoroughly.

In conclusion, the formation of high-field SABRE is reported allowing real-time *in situ* studies of polarization kinetics to be performed. The effect is consistent with a SPINOE-type<sup>2,23,26</sup> mechanism of nuclear spin cross-relaxation and polarization transfer to the Py substrate, although this conclusion is tentative and would certainly require further studies in the future. The mechanism is clearly different from that of the low-field SABRE. Furthermore, because at least a small fraction of the substrate undergoes chemical modification in the reaction with parahydrogen under our conditions, this process cannot rigorously be referred to as an exclusively non-hydrogenative PHIP. While the magnitude of the enhancement factors of high-field SABRE shown here is significantly smaller (up to 14.7 for pyridine and >100 for orthohydrogen and metal dihydride) than those typically observed with low-field SABRE (e.g., Figure 1), it is still quite pronounced, and optimization of this high-field effect may allow NMR signal enhancements without field cycling for some applications. Finally, hyperpolarized orthohydrogen and Ir hydride are likely intimately involved in the high-field SABRE mechanism; more generally, the presence of such highly polarized species in addition to the substrate should be accounted for in low-field detection, where chemical shift dispersion is negligible.<sup>17,31</sup>

## ■ ASSOCIATED CONTENT

### ● Supporting Information

Ir complex preparation and NMR spectra. This material is available free of charge via the Internet at <http://pubs.acs.org>.

## ■ AUTHOR INFORMATION

### Corresponding Author

eduard.chekmenev@vanderbilt.edu

### Notes

The authors declare no competing financial interest.

## ■ ACKNOWLEDGMENTS

This work was supported by the RAS (5.1.1), RFBR (14-03-00374-a, 14-03-31239-mol-a, 12-03-00403-a), SB RAS (57, 60, 61, 122), the Ministry of Education and Science of the Russian Federation, and the grants MK-4391.2013.3, NIH ICMIC SP50 CA128323-03, 5R00 CA134749-03, 3R00CA134749-02S1, DoD CDMRP W81XWH-12-1- 265 0159/BC112431.

## ■ REFERENCES

- (1) Golman, K.; Axelsson, O.; Johannesson, H.; Mansson, S.; Olofsson, C.; Petersson, J. *S. Magn. Reson. Med.* **2001**, *46*, 1.
- (2) Goodson, B. M. *J. Magn. Reson.* **2002**, *155*, 157.
- (3) Ardenkjaer-Larsen, J. H.; Fridlund, B.; Gram, A.; Hansson, G.; Hansson, L.; Lerche, M. H.; Servin, R.; Thaning, M.; Golman, K. *Proc. Natl. Acad. Sci. U.S.A.* **2003**, *100*, 10158.
- (4) Koptuyug, I. V.; Kovtunov, K. V.; Burt, S. R.; Anwar, M. S.; Hilty, C.; Han, S. I.; Pines, A.; Sagdeev, R. Z. *J. Am. Chem. Soc.* **2007**, *129*, 5580.
- (5) Day, S. E.; Kettunen, M. I.; Gallagher, F. A.; Hu, D. E.; Lerche, M.; Wolber, J.; Golman, K.; Ardenkjaer-Larsen, J. H.; Brindle, K. M. *Nat. Med.* **2007**, *13*, 1382.

- (6) Gallagher, F. A.; Kettunen, M. I.; Hu, D. E.; Jensen, P. R.; in't Zandt, R.; Karlsson, M.; Gisselsson, A.; Nelson, S. K.; Witney, T. H.; Bohndiek, S. E.; Hansson, G.; Peitersen, T.; Lerche, M. H.; Brindle, K. M. *Proc. Natl. Acad. Sci. U.S.A.* **2009**, *106*, 19801.

- (7) Kurhanewicz, J.; Vigneron, D. B.; Brindle, K.; Chekmenev, E. Y.; Comment, A.; Cunningham, C. H.; DeBerardinis, R. J.; Green, G. G.; Leach, M. O.; Rajan, S. S.; Rizi, R. R.; Ross, B. D.; Warren, W. S.; Malloy, C. R. *Neoplasia* **2011**, *13*, 81.

- (8) Nikolou, P.; Coffey, A. M.; Walkup, L. L.; Gust, B. M.; Whiting, N.; Newton, H.; Barcus, S.; Muradyan, I.; Dabaghyan, M.; Moroz, G. D.; Rosen, M.; Patz, S.; Barlow, M. J.; Chekmenev, E. Y.; Goodson, B. M. *Proc. Natl. Acad. Sci. U.S.A.* **2013**, *110*, 14150.

- (9) Abagam, A.; Goldman, M. *Rep. Prog. Phys.* **1978**, *41*, 395.

- (10) Walker, T. G.; Happer, W. *Rev. Mod. Phys.* **1997**, *69*, 629.

- (11) Eischmid, T. C.; Kirss, R. U.; Deutsch, P. P.; Hommeltoft, S. I.; Eisenberg, R.; Bargon, J.; Lawler, R. G.; Balch, A. L. *J. Am. Chem. Soc.* **1987**, *109*, 8089.

- (12) Bowers, C. R.; Weitekamp, D. P. *J. Am. Chem. Soc.* **1987**, *109*, 5541.

- (13) Adams, R. W.; Aguilar, J. A.; Atkinson, K. D.; Cowley, M. J.; Elliott, P. I. P.; Duckett, S. B.; Green, G. G. R.; Khazal, I. G.; Lopez-Serrano, J.; Williamson, D. C. *Science* **2009**, *323*, 1708.

- (14) Atkinson, K. D.; Cowley, M. J.; Elliott, P. I. P.; Duckett, S. B.; Green, G. G. R.; Lopez-Serrano, J.; Whitwood, A. C. *J. Am. Chem. Soc.* **2009**, *131*, 13362.

- (15) Crabtree, R. H.; Lavin, M.; Bonneviot, L. *J. Am. Chem. Soc.* **1986**, *108*, 4032.

- (16) Vazquez-Serrano, L. D.; Owens, B. T.; Buriak, J. M. *Inorg. Chim. Acta* **2006**, *359*, 2786.

- (17) Glogglar, S.; Muller, R.; Colell, J.; Emondts, M.; Dabrowski, M.; Blumich, B.; Appelt, S. *Phys. Chem. Chem. Phys.* **2011**, *13*, 13759.

- (18) Cowley, M. J.; Adams, R. W.; Atkinson, K. D.; Cockett, M. C. R.; Duckett, S. B.; Green, G. G. R.; Lohman, J. A. B.; Kerssebaum, R.; Kilgour, D.; Mewis, R. E. *J. Am. Chem. Soc.* **2011**, *133*, 6134.

- (19) Zeng, H.; Xu, J.; Gillen, J.; McMahon, M. T.; Artemov, D.; Tyburn, J.-M.; Lohman, J. A. B.; Mewis, R. E.; Atkinson, K. D.; Green, G. G. R.; Duckett, S. B.; van Zijl, P. C. M. *J. Magn. Reson.* **2013**, *237*, 73.

- (20) Feng, B.; Coffey, A. M.; Colon, R. D.; Chekmenev, E. Y.; Waddell, K. W. *J. Magn. Reson.* **2012**, *214*, 258.

- (21) Pravdivtsev, A. N.; Yurkovskaya, A. V.; Vieth, H.-M.; Ivanov, K. L.; Kaptein, R. *ChemPhysChem* **2013**, *14*, 3327.

- (22) Borowiak, R.; Schwaderlapp, N.; Huethel, F.; Lickert, T.; Fischer, E.; Bär, S.; Hennig, J.; Elverfeldt, D.; Hövener, J.-B. *Magn. Reson. Mater. Phys.* **2013**, *26*, 491.

- (23) Song, Y. Q. *Concept. Magnetic Res.* **2000**, *12*, 6.

- (24) van Weerdenburg, B. J. A.; Glogglar, S.; Eshuis, N.; Engwerda, A. H. J.; Smits, J. M. M.; de Gelder, R.; Appelt, S.; Wymenga, S. S.; Tessari, M.; Feiters, M. C.; Blumich, B.; Rutjes, F. P. J. T. *Chem. Commun.* **2013**, *49*, 7388.

- (25) Pavlik, J. W.; Laohhasurayotin, S. J. *Heterocycl. Chem.* **2007**, *44*, 1485.

- (26) Navon, G.; Song, Y. Q.; Room, T.; Appelt, S.; Taylor, R. E.; Pines, A. *Science* **1996**, *271*, 1848.

- (27) Oddershede, J.; Geertsen, J.; Scuseria, G. E. *J. Phys. Chem.* **1988**, *92*, 3056.

- (28) Rubottom, G. M.; Evain, E. J. *Tetrahedron* **1990**, *46*, 5055.

- (29) Gröll, B.; Schnürch, M.; Mihovilovic, M. D. *J. Org. Chem.* **2012**, *77*, 4432.

- (30) Theis, T.; Ledbetter, M. P.; Kervern, G.; Blanchard, J. W.; Ganssle, P. J.; Butler, M. C.; Shin, H. D.; Budker, D.; Pines, A. *J. Am. Chem. Soc.* **2012**, *134*, 3987.

- (31) Gong, Q. X.; Gordji-Nejad, A.; Blumich, B.; Appelt, S. *Anal. Chem.* **2010**, *82*, 7078.

- (32) Fulmer, G. R.; Miller, A. J. M.; Sherden, N. H.; Gottlieb, H. E.; Nudelman, A.; Stoltz, B. M.; Bercaw, J. E.; Goldberg, K. I. *Organometallics* **2010**, *29*, 2176.